HHS Public Access

Author manuscript

Biochim Biophys Acta. Author manuscript; available in PMC 2022 May 03.

Published in final edited form as:

Biochim Biophys Acta. 2012 May ; 1817(5): 792–801. doi:10.1016/j.bbabio.2012.01.004.

Net light-induced oxygen evolution in photosystem I deletion mutants of the cyanobacterium *Synechocystis* sp. PCC 68031

Qing Jun Wang[2,3], **Abhay Singh**[4,5], **Hong Li**[4,6], **Ladislav Nedbal**[7], **Louis A. Sherman**[4], **Govindjee**[2,8,10,9], **John Whitmarsh**[2,8,11]

[2]Center for Biophysics & Computational Biology, University of Illinois at Urbana-Champaign, Urbana, IL 61801, USA (Q.J.W., Govindjee, J.W.)

[4]Department of Biological Sciences, Purdue University, Lilly Hall, West Lafayette, IN 47907, USA (A.S., H.L., L.A.S.)

[7]Institute of Systems Biology and Ecology AVCR and Institute of Physical Biology JU, Zámek 136, CZ-37333 Nové Hrady, Czech Republic (L.N.)

[8]Department of Plant Biology, University of Illinois at Urbana-Champaign, Urbana, IL 61801, USA (Govindjee, J.W.)

[10]Department of Biochemistry, University of Illinois at Urbana-Champaign, Urbana, IL 61801, USA (Govindjee)

[11]USDA/ARS (J.W.)

Abstract

Oxygenic photosynthesis in cyanobacteria, algae, and plants requires photosystem II (PSII) to extract electrons from H_2O and depends on photosystem I (PSI) to reduce $NADP^+$. Here we demonstrate that mixotrophically-grown mutants of the cyanobacterium *Synechocystis* sp. PCC 6803 that lack PSI (ΔPSI) are capable of net light-induced O_2 evolution *in vivo*. The net light-induced O_2 evolution requires glucose and can be sustained for more than 30 minutes. Utilizing electron transport inhibitors and chlorophyll *a* fluorescence measurements, we show that in these mutants PSII is the source of the light-induced O_2 evolution, and that the plastoquinone pool is reduced by PSII and subsequently oxidized by an unidentified electron acceptor that does not involve the plastoquinol oxidase site of the cytochrome b_6f complex. Moreover, both O_2 evolution and chlorophyll *a* fluorescence kinetics of the ΔPSI mutants are highly sensitive to

[1]This work was supported by the USDA/Agricultural Research Service (J.W.), grant-FG02-99ER20342 from DOE (L.A.S), and grants MSM6007665808 from MSMT and AV0Z60870520 from USBE AVCR (L.N).

[3]Corresponding author. Qing Jun Wang, Department of Molecular and Cellular Biochemistry, University of Kentucky, College of Medicine, B163 BBSRB, 741 South Limestone, Lexington, KY 40536-0509, USA; qingjun.wang@uky.edu. [9]Corresponding author. Govindjee, Department of Plant Biology, University of Illinois at Urbana-Champaign, 265 Morrill Hall, 505 South Goodwin Avenue, Urbana, Illinois, 61801, USA; gov@illinois.edu.

[5]Current address: MOgene Green Chemicals, 4633 World Parkway Circle, Saint Louis, MO 63134, USA; e-mail: asingh@mogene.com

[6]Current address: VaxInnate Corporation, 3 Cedar Brook Dr., Cranbury, NJ 08512, USA; hli710@yahoo.com

KCN, indicating the involvement of a KCN-sensitive enzyme(s). Experiments using ^{14}C-labeled bicarbonate show that the ΔPSI mutants assimilate more CO_2 in the light compared to the dark. However, the rate of the light-minus-dark CO_2 assimilation accounts for just over half of the net light-induced O_2 evolution rate, indicating the involvement of unidentified terminal electron acceptors. Based on these results we suggest that O_2 evolution in ΔPSI cells can be sustained by an alternative electron transport pathway that results in CO_2 assimilation and that includes PSII, the platoquinone pool, and a KCN-sensitive enzyme.

1. Introduction

The light-driven reactions of photosynthesis in cyanobacteria, algae, and plants are described by a Z-scheme, the linear electron transport pathway from H_2O to ferredoxin (Fd) and $NADP^+$ that generates O_2 as a byproduct and drives the assimilation of CO_2[1–3]. This linear electron transport pathway depends on photosystem II (PSII)[4], photosystem I (PSI) [5] and the cytochrome b_6f (Cyt bf) complex[6]. Although the Z-scheme serves as the dominant pathway in oxygenic photosynthesis, PSII-driven electron transport from H_2O without the involvement of PSI has been suggested[7–10]. Govindjee *et al.*[7] proposed an alternative electron transport pathway in algal cells in which PSII could reduce $NADP^+$ independent of PSI — a pathway similar to that in photosynthetic bacteria. Arnon ([9] and the references therein) proposed a more complicated pathway for the reduction of Fd by PSII — a pathway that required plastocyanin, but not PSI. Several PSI deletion mutants of *Chlamydomonas reinhardtii* have been shown to evolve O_2 in the light[11–13]. However, the rate of light-induced O_2 evolution in these mutants was lower than that of respiration, resulting in net O_2 uptake. In addition, neither CO_2 assimilation nor H_2 production was observed in these mutants.

The observation of net light-induced O_2 evolution in the absence of PSI was first reported in two PSI deletion mutants (ΔPSI) of the cyanobacterium *Synechocystis* sp. PCC 6803 ([8] and L. B. Smart, personal communication). Smart et al.[8] speculated that the plastoquinone (PQ) pool, $NADP^+$, H^+ and/or O_2 may serve as the terminal electron acceptor(s) for the PSI-independent O_2 evolution. Additional ΔPSI mutants of *Synechocystis* 6803 have been generated in the laboratories of Himadri Pakrasi (Washington University, St. Louis, MO) and Wim F. J. Vermaas (Arizona State University, Tempe, AZ)[14–17]. Vermaas and co-workers (see e.g.[18–20]) proposed PSII-driven electron transfer from H_2O to O_2 via a pathway that involved PQ and potassium cyanide (KCN)-sensitive respiratory terminal oxidases. However, Vermaas and co-workers did not observe net light-induced O_2 evolution in the absence of PSI.

In the present work, we report that in several mixotrophically-grown ΔPSI mutants of *Synechocystis* 6803, the rate of PSII water oxidation in the light in the presence of glucose and $NaHCO_3$ is significantly faster than the respiration rate, resulting in net O_2 evolution. Inhibitor studies and chlorophyll (Chl) *a* fluorescence measurements demonstrate the presence of electron transport from H_2O to the PQ pool and the involvement of KCN-sensitive enzyme(s) in the ΔPSI mutants. We show that although the ΔPSI mutants are

capable of light-minus-dark CO_2 assimilation, the rate is about half of that required to account for the rate of net O_2 evolution.

2. Materials and methods

2.1. Mutants and growth conditions

The glucose tolerant wild type (WT) strain of *Synechocystis* sp. PCC 6803 and six PSI deletion mutant strains were gifts from Himadri Pakrasi (E. Zak and H. Pakrasi, personal communication) and W. F. J. Vermaas[14–17]. Details of these mutants are summarized in Table 1. These cyanobacterial strains were maintained according to the methods provided by the laboratories donating the strains. The antibiotics and glucose concentrations used for the BG-11 plates were as follows: 50 μg/ml kanamycin and 10 mM glucose for ΔAB; 25 μg/ml spectinomycin and 10 mM glucose for ΔVIII–XI; 25 μg/ml chloramphenicol and 15 mM glucose for ΔPSI/WV; 10 μg/ml erythromycin, 25 μg/ml chloramphenicol and 15 mM glucose for ΔPSIΔApcE; 15 μg/ml zeocin, 25 μg/ml erythromycin, 35 μg/ml chloramphenicol, 25 μg/ml spectinomycin and 15 mM glucose for ΔPSIΔNdbABC; 25 μg/ml erythromycin, 35 μg/ml chloramphenicol, 25 μg/ml spectinomycin and 15 mM glucose for ΔPSI ΔCtaDIIEII ΔCydAB.

The WT cells were cultured in the BG-11 medium in the presence or the absence of 5 mM glucose at 30°C under 65 μmol photons·m^{-2}·s^{-1} fluorescent light. All of the ΔPSI mutant strains were grown in the presence of 5 mM glucose at 30°C without antibiotics. All of the ΔPSI mutant strains except for the ΔPSIΔApcE strain were grown under ca. 1.5 μmol photons·m^{-2}·s^{-1} fluorescent light. The ΔPSIΔApcE strain was grown under 65 μmol photons·m^{-2}·s^{-1} fluorescent light. The cell cultures were bubbled with water-saturated air through a sterilized filter (Gelman #4210, 0.3 μm pore size). Cells were grown in the BG-11 medium either with or without the supplement of 1 μM Cu^{2+} (in the form of $CuSO_4$), which has been previously reported to be sufficient for these cells to express either plastocyanin or Cyt c_6, respectively[21]. The absence of plastocyanin in the cells grown without the Cu^{2+} supplement* was indirectly examined by the presence of the light-minus-dark absorption peak of Cyt c_6 at 553 nm. The cell density was monitored by measuring the optical density of the cell cultures at 730 nm[22].

2.2. Measuring the net light-induced O_2 evolution and dark respiration rates and the PSII activity

Cells were harvested during exponential growth phase by centrifugation at 5,000 g for 5 min at room temperature and kept in fresh BG-11 medium in the presence of 5 mM glucose (unless noted otherwise) prior to the measurements. This glucose concentration was sufficient for maintaining the activities during the measurements. Based on the growth curves, it was also sufficient to sustain cell growth until stationary phase. The rates of the net light-induced O_2 evolution and the dark respiration of whole cells were monitored at 30°C by a Clark-type electrode (YSI 5331 oxygen probe, Yellow Springs, OH) with a polarizing voltage of −0.7 volts[23–24]. The actinic light was provided by a pair of Tungsten-halogen

*No special procedure was employed to remove trace amounts of Cu^{2+}.

lamps (EG&G, 250 W) illuminating from both sides of the reaction chamber after being filtered through pairs of heat-reflecting filters (Melles Griot 03MHG007), heat absorbing blocking filters (Corning CS I–75, Rochester, NY), red blocking filters (Corning CS 2–63, Rochester, NY) and appropriate neutral density filters. The light intensity for reaching maximal net O_2 evolution rate was measured to be 500 μmol photons·m^{-2}·s^{-1} (same on each side) by a Licor Quantum Photometer LI-185B (Lincoln, NE). Sodium dithionite was used to calibrate the electrode. $NaHCO_3$ was added at 10 mM concentration to the cell suspensions in the reaction chamber right before the measurements.

For testing 2,5-dibromo-3-methyl-6-isopropyl-*p*-benzoquinone (DBMIB) adaptation, the WT cells were also grown in the presence of micromolar DBMIB and 5 mM glucose under ca. 1.5 μmol photons·m^{-2}·s^{-1} light intensity for a total of two inoculation cycles: the concentration of DBMIB on the day of each inoculation was 10 μM; an extra dose of DBMIB (equivalent to 2 μM final concentration) was supplied everyday afterwards to compensate for the light-sensitive loss of DBMIB. For titrating the net O_2 evolution rates of these DBMIB-adapted cells with DBMIB, the cells were washed with fresh BG-11 three times to remove DBMIB that was present during the cultivation.

The PSII activity was measured as the saturation light-induced O_2 evolution rate in the presence of artificial PSII electron acceptors (i.e., 1.2 mM potasium ferricyanide (FeCN) and 600 μM 2,6-dichloro-*p*-benzoquinone (DCBQ)) and with the saturated actinic light intensity as high as 3,600 μmol photons·m^{-2}·s^{-1}.

2.3. Membrane preparation

Membranes from the *Synechocystis* 6803 cells were prepared as previously described[25] with minor modifications. All steps were carried out at 4 °C. The cell pellet from 50 ml cell culture was re-suspended in 1 ml breakage buffer containing 50 mM HEPES/NaOH (pH 7), 0.5 M sucrose, 15 mM NaCl, 5 mM $MgCl_2$, 0.1% (v/v) Protease Inhibitor Cocktail (Sigma), and 4 μg/mL DNase I. These cells were broken by glass beads (size 150~212 microns, acid-washed, Sigma) with 5 cycles of 2 min of vortexing followed by 2 min of cooling on ice. After the final cycle, the glass beads were allowed to settle and the homogenate was collected. The glass beads were washed several times and the homogenates were pooled. Debris spin was carried out at 8,160 g (Eppendorf, model Centrifuge 5415C) for 5 min. The supernatant was collected and centrifuged again at 16,000 g for 30 min. The membrane pellet was collected and re-suspended in the breakage buffer.

2.4. Chl concentration, Chl-to-PSII ratio and PSII concentration determination

Concentration of Chl in *Synechocystis* 6803 cells was spectrophotometrically determined[26]. The Chl-to-PSII ratios of the membrane preparations were determined by measuring their O_2 evolution activity driven by single-turnover flashes[23]. The actinic light was provided by 600 flashes (frequency 10 Hz, width 6 μs) of a Xe-flash lamp (FX-200; EG&G, Salem, MA). The actinic flashes were filtered by a yellow filter (Corning CS 3–71, Rochester, NY) and 1 cm of water. The Xe-flash lamp was driven by 700 V to yield saturating light intensity. The O_2 evolution rate of the membranes was measured at 30°C using a Clark-type oxygen electrode, as described in section 2.2. The reaction buffer

contained 50 mM MES-NaOH (pH 6.0), 10 mM $MgCl_2$, 5 mM $CaCl_2$, 5 mM NaCl and 0.5 M sucrose. The optimal O_2 evolution rate was reached when the reaction mixture contained 250 μM FeCN and 100 μM DCBQ. Varying the saturating single-turnover flash number between 400 and 800 or the flash frequency between 5 and 20 Hz had no effect on the O_2 evolution rate. When calculating the Chl-to-PSII ratios, we assumed that one O_2 molecule was evolved per PSII per four flashes. The PSII concentration of each sample was determined by converting the Chl concentration using corresponding Chl-to-PSII ratio. In our work, the net light-induced O_2 evolution rate and light-minus-dark CO_2 assimilation were calculated on a PSII basis, because the PSI-less mutants of *Synechocystis* 6803 had a much lower Chl-to-PSII ratio than WT. In WT, 80–85% of all Chl is associated with the PSI core complex, which is lost in the PSI-less mutants[15]. Because of the low Chl-to-PSII ratio, most PSI-less mutants could be grown only under low light, except for the ΔPSIΔApcE strain in which the light harvesting complex was impaired in addition to PSI.

2.5. The kinetics of PSI reaction center, P700

Flash-induced P700 oxidation and re-reduction kinetics of the membrane preparations were measured at room temperature using a laboratory-built single-beam spectrophotometer as described earlier[27]. The saturating single-turnover actinic flashes (width, 6 μs) were provided by a pair of Xe-flash lamps (FX-200; EG&G, Salem, MA) from both sides of the sample cuvette to induce a rapid oxidation of the PSI primary donor P700. The actinic flashes were filtered by two broad-band interference filters (DT-Blau, Balzers) and two blocking filters (Corning CS 4–96, Rochester, NY). The flash-induced P700 oxidation and re-reduction kinetics were recorded at discrete wavelengths ranging from 665 nm to 830 nm. Typically, at each wavelength, data from 8 runs were averaged. The reaction buffer for P700 measurements contained 50 mM Tris-HCl (pH 8.3), 33 μM 2,6-dichlorophenolindophenol (DCPIP), and 1.7 mM sodium ascorbate. Chl concentration was adjusted to be between 20~30 μM for best signal-to-noise ratio and to get desirable PSII concentration. The samples were stirred after measuring absorbance at each wavelength. The experiments were carried out at 24±1°C.

2.6. Chl *a* fluorescence kinetics

Chl *a* fluorescence kinetics was monitored using a dual-modulation kinetic fluorometer (PSI, Brno, Czech Republic). The single-turnover, saturating flashes were provided by diodes (LEDs) emitting at 660 nm. The measuring flashes were provided by LEDs emitting at 620 nm[28]. Cells at exponential growth phase were resuspended in fresh BG-11 medium in the presence of 5 mM glucose. The cell density was adjusted so that Chl concentration was ca. 1 μM for best signal-to-noise ratio. Cells were dark adapted for 10 min before each experiment. For measuring the Chl *a* fluorescence induction kinetics, three data points (1 ms apart) were collected in darkness for measuring the F_0 level. Afterwards, a train of 5,000 saturating, single-turnover flashes were fired at 1 kHz for 5 s. For measuring the Chl *a* fluorescence dark relaxation kinetics, the actinic light was turned off at 370 ms when the Chl *a* fluorescence reached the maximum, and subsequently the redox states of Q_A^- and the PQ pool were probed for ca. 20 s by logarithmically spaced measuring flashes. The duration and intensity of the measuring flashes were adjusted to minimize their actinic effect. The experiments were carried out at 24±1°C.

2.7. Measurements of the CO_2 assimilation rates

The CO_2 assimilation rates were measured using ^{14}C-labeled $NaHCO_3$[29]. Cells at the exponential growth phase were harvested. The cell pellet was re-suspended in freshly prepared HCO_3^--less BG-11 medium. $NaH^{14}CO_3$ was diluted with cold $NaHCO_3$. The final $NaHCO_3$ concentration in the reaction mixtures was either 5 mM or 10 mM for several independent experiments. An aliquot of 0.85 ml cell suspension combined with 0.85 ml diluted $NaH^{14}CO_3$ was used for O_2 evolution measurement and another aliquot was kept in the dark as the control. After the O_2 evolution measurement, both the sample and the control were quickly treated with a strong acidic solution containing 0.7 ml of 4 M formic acid and 1 M HCl to break the cells in order to release un-incorporated inorganic carbon. Both the sample and the control were dried overnight in the hood at 65°C with air blowing over them. Then 0.5 ml of 0.1 M HCl was added to each vial to dissolve the organic forms of carbon. After addition of the scintillation cocktail to the sample, radioactivity of the sample was counted in a liquid scintillation counter (liquid scintillation analyzer, Packard, model tri-carb 1600tr). The specific activity was calculated from three replicas of the diluted $NaH^{14}CO_3$ aliquots. The calculated specific activities for these experiments ranged from 200 to 1,000 cpm/nmole $NaH^{14}CO_3$.

3. Results

3.1. Spectroscopic measurements confirm the absence of PSI activity in *Synechocystis* 6803 mutant strains lacking PSI

We characterized six ΔPSI mutants, which were generated in the laboratories of Himadri Pakrasi and Wim F. J. Vermaas (Table 1). In each of these mutants, a significant portion of either the *psaB* gene (encoding for the PSI core protein PsaB) or the *psaAB* operon (encoding for the PSI core proteins PsaA and PsaB) was replaced by an antibiotic resistance marker. These ΔPSI mutant strains were completely segregated and the absence of PSI was confirmed in their original laboratories by Southern and Western blots (E. Zak and H. Pakraski, personal communication and[14–17]) (see discussion in Supplemental Material S1). We further examined the absence of PSI in these mutant strains by measuring their P700 oxidation and re-reduction kinetics. When a saturating single-turnover flash was applied to the WT membranes, a large absorbance change reflecting a rapid light-induced oxidation of P700 (peak 703 nm), followed by its re-reduction in the dark, was observed. In contrast, such P700 oxidation transient was not detected in the membranes prepared from the ΔPSI (ΔAB) mutant (Fig. 1A). To determine the detection limit of our instrument, we ‘titrated’ the ΔAB membranes with small amounts of the WT membranes. As shown in Fig. 1B, the light-induced absorbance change resulting from as little as 1% WT P700 oxidation (on a PSII basis) can be detected with our instrument. Therefore, within a maximal experimental error of 1%, there was no detectable PSI activity in the ΔAB mutant. Similar conclusions were reached with the other ΔPSI strains, where there was no detectable PSI activity within maximal experimental errors of 1–5% (data not shown).

3.2. ΔPSI mutants show net light-induced O_2 evolution in the presence of glucose and $NaHCO_3$

Despite the lack of PSI, all the ΔPSI cells showed a net light-induced O_2 evolution *in vivo* in the presence of 5 mM glucose and 10 mM $NaHCO_3$ **. For example, Fig. 2 shows a representative chart recorder trace of net light-induced O_2 evolution in the ΔAB cells that was sustained for 30 min. The trace, which is similar to that for the other mutants, shows a net O_2 uptake in the dark due to respiration, followed by a net oxygen evolution in the light, indicating that the rate of light-induced O_2 evolution exceeds the rate of respiration in the light.

Here we define the net light-induced O_2 evolution rate (i.e., the observed O_2 evolution rate, not adjusted for respiration) as P_{obs}, the dark respiration rate (i.e., O_2 consumption rate, of positive values) as R, and the O_2 evolution rate that is adjusted for dark respiration as P_{adj} (Fig. 2). Thus $P_{adj} = R + P_{obs}$, assuming the respiration rate in the light was the same as that in the darkness***. Classically, O_2 evolution rate is calculated as P_{adj} with the above assumption. We note that O_2 uptake in the light could also be inhibited (e.g., "Kok effect") or stimulated (e.g., as reported in another cyanobacterium *Synechococcus elongatus* at medium and high light intensities[30]) in the ΔPSI cells. Therefore, in this work, we primarily used P_{obs} as the readout for O_2 evolution. As summarized in Table 2, on a PSII basis, the net light-induced O_2 evolution rate P_{obs} was 4±1 mol O_2·mol $PSII^{-1}$·s^{-1} in the PSI deleted ΔAB cells, amounting to about 13% of that in the WT cells (34±5 mol O_2·mol $PSII^{-1}$·s^{-1}); the dark respiration rate R was 6±2 mol O_2·mol $PSII^{-1}$·s^{-1} in the ΔAB cells, similar to that in the WT cells (5±1 mol O_2·mol $PSII^{-1}$·s^{-1}); and P_{adj} was 10±3 mol O_2·mol $PSII^{-1}$·s^{-1} in the ΔAB cells, amounting to about 26% of that in the WT cells (39±5 mol O_2·mol $PSII^{-1}$·s^{-1}). Similarly, significant net light-induced O_2 evolution was also observed in all other ΔPSI strains tested (e.g., the net light-induced O_2 evolution rates were 4±1 mol O_2·mol $PSII^{-1}$·s^{-1} in ΔPSIΔNdbABC and 2.2±0.4 mol O_2·mol $PSII^{-1}$·s^{-1} in ΔPSIΔCtaDIIEIIΔCydAB). Our data are consistent with the previous observation of net light-induced O_2 evolution in the absence of supplemental electron acceptors for either the *psaA*- or the *psaB*-deletion mutant of *Synechocystis* 6803 – the ADK9[8] or BDK8 (L. B. Smart 2006, personal communication) strains.

The significant amount of net light-induced O_2 evolution of the ΔPSI mutants suggests the existence of alternative electron transport pathway(s) downstream of oxygenic PSII water oxidation in the absence of PSI. This net light-induced O_2 evolution in the ΔPSI mutants also indicated that the electron sinks of the alternative electron transport pathways in the absence of PSI are not limited to O_2, which has previously been suggested to be a sink for the PSII-generated electrons via a respiratory terminal oxidase in the ΔPSI/WV mutant[19–20].

**In the present work, both O_2 and CO_2 were monitored in the presence of 5 mM glucose and 10 mM $NaHCO_3$ unless stated otherwise.

***In the formula $P_{adj} = R + P_{obs}$, respiration (R) is positive.

3.3. O_2 evolution in the absence of PSI requires glucose

Synechocystis sp. PCC 6803 is known to be a facultative photoheterotroph in the presence of glucose[31–32]. Consistent with this observation, we found that the PSI deleted ΔAB mutant did not grow either photoautotrophically or mixotrophically with non-glucose carbon sources such as sucrose, fructose, glycerol or mannose. We next examined whether glucose was required to sustain O_2 evolution in the ΔAB cells. We found that upon depleting glucose from the medium, P_{obs} (Fig. 3A), R (Fig. 3B) and P_{adj} (Fig. 3C) dropped gradually to basal levels with similar time constants (ca. 8 h). After 42 h of glucose depletion, we added 5 mM glucose back to the ΔAB cell culture. While respiration recovered almost instantly, the net light-induced O_2 evolution P_{obs} was restored slowly and partially (Fig. 3D). In contrast, adding back non-metabolic glucose analogs, including 3-*O*-methyl glucose and 2-deoxy glucose, was not effective in restoring either the net light-induced O_2 evolution or the dark respiration of the glucose-depleted ΔAB cells. These results suggest the requirement of glucose and/or its metabolite(s) for sustaining the net light-induced O_2 evolution in the absence of PSI. In addition, after incubating the ΔAB cells with added glucose for ca. 30 min, we re-deprived these cells of glucose. Again, P_{obs}, R and P_{adj} dropped gradually to basal levels. However, the decay of these rates during the second glucose deprivation was much faster (ca. 10 min) than that during the first glucose deprivation (ca. 8 h), suggesting depletion of the unidentified electron sinks as a result of the prior prolonged glucose deprivation. To further characterize the net light-induced O_2 evolution of the mixotrophically-grown ΔPSI mutants of *Synechocystis* 6803, we examined whether several known linear electron transport pathway components were involved and whether the ΔPSI mutants were capable of CO_2 assimilation, as will be described below in sections 3.4 to 3.8.

3.4. PSII is the source of O_2 evolution in the absence of PSI

To examine the involvement of PSII in O_2 evolution in the absence of PSI, we titrated the ΔPSI cells with the PSII inhibitor, 3-(3,4-dichlorophenyl)-1,1-dimethylurea (DCMU). We found that oxygen evolution was completely inhibited in the ΔPSI cells by 10 μM DCMU, while respiration was insensitive. This observation is consistent with the reported DCMU sensitivity of O_2 evolution in the ΔPSI mutant strain ADK9[8]. The observed DCMU sensitivity of O_2 evolution in the ΔPSI cells was similar to that in the WT cells (I_{50} ~ 100 nM for both), suggesting that O_2 evolution of the ΔPSI cells originated from oxygenic PSII water oxidation.

To directly assess the PSII activity in the absence of PSI, we measured the light-induced O_2 evolution rate of the ΔAB cells in the presence of the artificial PSII electron acceptors DCBQ and FeCN. The PSII activity of the ΔAB cells (110 mol O_2·mol $PSII^{-1}$·s^{-1}) was comparable to that of the WT cells (66 mol O_2·mol $PSII^{-1}$·s^{-1}) (Table 2). This result is consistent with the reported similarity of the light-induced O_2 evolution rates (on a per cell basis) in the presence of 1 mM DCBQ between the WT and the ΔPSI mutant (ADK9) strains[8], suggesting un-impaired PSII in the ΔPSI cells.

To characterize PSII activity in the ΔPSI cells, we monitored Chl *a* fluorescence induction kinetics (the Kautsky effect)[33–34]. Chl *a* fluorescence emission yield reflects the redox state of Q_A, the first PQ electron acceptor in PSII: It increases with the reduction of Q_A and

decreases with the oxidation of Q_A^-[35–36]. In the absence of DCMU, hundreds of ms of illumination was required to reduce Q_A and the PQ pool to reach fluorescence maxima F_P ($\approx F_M$) (Fig. 4A, closed symbols; ca. 170 ms in WT, ca. 320 ms in the ΔAB cells, and ca. 560 ms in the ΔPSIΔApcE cells). In contrast, in the presence of DCMU, Q_A was fully reduced to give maximal Chl *a* fluorescence emission yield (F_M) within 2 ms of illumination by actinic flashes (Fig 4A, open symbols). These results show that DCMU has the same effect on Chl *a* fluorescence induction kinetics in the WT cells (Fig 4A, circles) and ΔPSI cells (Fig 4A, squares and triangles), demonstrating the PSII-origin of O_2 evolution in the ΔPSI cells. Furthermore, these results indicate that the lower net light-induced O_2 evolution observed the ΔPSI cells compared to that in the WT cells, is the result of a limitation in electron transport downstream from PSII, rather than an impaired PSII capacity.

3.5. The PQ pool is involved in O_2 evolution of the ΔPSI cells

To investigate the involvement of the PQ pool in O_2 evolution, we monitored the oxidation kinetics of Q_A^- and the plastoquinol (PQH_2) pool in the WT and ΔPSI (ΔAB and ΔPSIΔApcE) cells by recording their Chl *a* fluorescence dark relaxation kinetics after their Q_A and the PQ pool were reduced (Fig. 4B). In the presence of 10 μM DCMU, Chl *a* fluorescence of the WT and the ΔPSI cells relaxed slowly in the darkness with the same time constant $T^{DCMU} \approx 1$ s (Fig. 4B, open symbols). This slow Chl *a* fluorescence dark relaxation kinetics in the presence of DCMU was also reported previously in the ΔPSI/WV cells and is attributed to the Q_A^- oxidation through the back reaction of PSII[20].

In contrast, in the absence of DCMU, the Chl *a* fluorescence dark relaxation curves of the WT and ΔPSI mutants were significantly different (Fig. 4B, closed symbols): The relaxation kinetics were biphasic in the WT cells (Fig. 4B, closed circles) with time constants of $T_{slow}^{WT} = 0.1–1$ s and $T_{fast}^{WT} \approx 1–10$ ms, respectively, whereas the relaxation kinetics of both the ΔAB (Fig. 4B, closed squares) and the ΔPSIΔApcE (Fig. 4B, closed triangles) cells were monophasic with an intermediate time constant of $T^{\Delta PSI} \approx 10–100$ ms. The slow phase of the Chl *a* fluorescence dark relaxation kinetics in the WT cells in the absence of DCMU is attributed to the Q_A^- oxidation through the back reaction of PSII[20]. Alternatively, it may reflect the cyclic electron transport around PSI which reduces the PQ pool[37–38]. The fast phase of Chl *a* fluorescence dark relaxation kinetics in the WT cells in the absence of DCMU indicates a more oxidized PQ pool as a result of the PSI activity before the actinic light is switched off. In contrast, the intermediately-fast time constant of the monophasic Chl *a* fluorescence dark relaxation kinetics in the ΔPSI cells in the absence of DCMU reflects a more reduced PQ pool, possibly as a result of less effective PQH_2 oxidation pathway(s) than PSI.

These observations show that the PQ pool is involved in O_2 evolution in the ΔPSI cells, and that PQH_2-oxidizing pathway(s) other than PSI must exist to sustain the prolonged O_2 evolution in the absence of PSI.

3.6. PQH_2 oxidation in the ΔPSI cells does not involve the Q_o site of the Cyt bf complex

At low concentrations (≤1 μM), DBMIB inhibits PQH_2 oxidation at the plastoquinol oxidase (Q_o) site of the Cyt bf complex[39], whereas at higher concentrations (≥10 μM), DBMIB

can inhibit Q_A^- oxidation in a DCMU-like manner (reviewed in[40]). To examine whether the Cyt bf complex could effectively oxidize PQH_2 in the absence of PSI, we titrated O_2 evolution of the ΔPSI cells with DBMIB. Our data show that O_2 evolution of the ΔPSI cells was much less sensitive to DBMIB than that of the WT cells. The DBMIB concentration leading to 50% inhibition (I_{50}) of the net O_2 evolution rate P_{obs} was 0.5 μM for the WT cells (Fig. 5A, closed circles) and 4.2 μM for the ΔPSI cells (Fig. 5A, open circles), respectively. Significantly different I_{50} values for the DBMIB inhibition of the adjusted O_2 evolution rate P_{adj} were also observed for the WT (0.6 μM; Fig. 5C, closed circles) and ΔPSI cells (23.7 μM; Fig. 5C, open circles). In contrast, the dark respiration rate R was not inhibited by DBMIB (50 μM) in either WT (Fig. 5B, closed circles) or ΔPSI (Fig. 5B, open circles) cells. These results indicate that the Q_o site of the Cyt bf complex is unlikely to be involved in the PQH_2-oxidizing pathway(s) that contributes to the net light-induced O_2 evolution in the ΔPSI cells.

3.7. Oxygen evolution in the ΔPSI cells is highly sensitive to KCN

Cyanide is a potent inhibitor of the respiratory cytochrome oxidase and other metalloproteins including plastocyanin[41] and Rubisco[42–43]. To examine the possible involvement of KCN-sensitive redox components in the PQH_2-oxidizing pathway(s) in the ΔPSI cells, we titrated O_2 evolution and dark respiration with KCN. Our data showed that P_{obs} of the ΔPSI cells was highly KCN-sensitive (I_{50} ~ 1.7 μM, Fig. 6A, open circles), as compared to that of the WT cells (I_{50} ~ 49 μM, Fig. 6A, closed circles). Similarly, P_{adj} of the ΔPSI cells was also highly KCN-sensitive (I_{50} ~ 6 μM, Fig. 6C, open circles), as compared to that of the WT cells (I_{50} ~ 46 μM, Fig. 6C, closed circles). In contrast, dark respiration of the ΔPSI cells was much less sensitive to KCN, with the I_{50} values of 30 μM in both the WT (Fig. 6B, closed circles) and ΔPSI (Fig. 6B, open circles) cells.

To further investigate the KCN-sensitive PQH_2-oxidizing pathway(s) in the ΔPSI cells, we examined the possible involvement of PSII, plastocyanin and respiratory terminal oxidases. By monitoring O_2 evolution in the presence of the artificial PSII electron acceptors FeCN and DCBQ, we found that the PSII activities of both the WT cells and the PSI deleted ΔAB cells were not inhibited by 500 μM KCN. Therefore, the KCN inhibition of both P_{obs} and P_{adj} of the WT and ΔPSI cells does not result from the KCN inhibition of PSII.

Plastocyanin has been previously shown to react readily with high concentrations of KCN (>10 mM)[41]. We grew the ΔPSI cells either in the presence or in the absence of 1 μM Cu^{2+} supplement so that they expressed either plastocyanin or Cyt c_6, respectively[21]. Both plastocyanin- and Cyt c_6-expressing cells exhibited indistinguishable KCN titration curves (Fig. 6), further supporting that the PQH_2-oxidizing pathway(s) in the absence of PSI does not involve plastocyanin.

Lastly, we monitored the KCN effect on Chl *a* fluorescence dark relaxation kinetics of the ΔPSI cells (Fig. 7A). Chl *a* fluorescence dark relaxation in the ΔPSI mutants was severely inhibited by 1.5 mM KCN (Fig. 7A, closed squares), as compared to without it (Fig. 7A, closed circles). Notably, Chl *a* fluorescence dark relaxation kinetics of the ΔPSI mutants in the presence of KCN (Fig. 7A, closed squares) was similar to that in the presence of DCMU (Fig. 7A, open circles), suggesting effective inhibition of the oxidation of Q_A^-

and the PQH_2 pool by KCN in the ΔPSI cells. In contrast, in the WT cells, KCN did not cause significant inhibition of the PQH_2 pool oxidation (Fig. 7B, closed squares); rather, it induced a small light-to-dark transient increase of the Chl *a* fluorescence yield which was previously attributed to the delayed reduction of the PQ pool by the KCN-independent cyclic electron transport around PSI[37–38]. In spite of the fact that KCN inhibits the oxidation of Q_A^- and the PQH_2 pool, which was previously attributed to the KCN-sensitive PQH_2-oxidizing activity of respiratory cytochrome oxidases in the ΔPSI/WV cells[20], we suggest that the KCN-sensitivity of the net light-induced O_2 evolution in the ΔPSI cells is independent of direct involvement of respiratory terminal oxidases (see the Discussion and the Supplemental Material S2). In addition, the observed KCN-sensitivity of the net light-induced O_2 evolution in the WT cells has an I_{50} value close to the reported I_{50} value for the cyanide inhibition of Rubisco[42–43]; thus, it may be attributed to the KCN inhibition of the Calvin-Benson cycle.

3.8. The ΔPSI cells are capable of light-minus-dark CO_2 assimilation in the presence of glucose

We examined CO_2 assimilation in the ΔPSI cells by performing *in vivo* radioisotope-labeling studies using $NaH^{14}CO_3$. Our data show that the ΔPSI cells took up CO_2 both in the darkness and upon illumination, resulting in significant amount of light-minus-dark CO_2 uptake (Table 2 and Fig. 8A). Since acid-stable intermediates instead of acid-labile carbamates of proteins or bicarbonate of carbon concentrating mechanism (CCM)[44–47] were monitored in these experiments, the observed CO_2 uptake in the ΔPSI cells was in fact CO_2 assimilation. The light-minus-dark CO_2 assimilation rate was measured to be 2.2±0.9 mol CO_2·mol $PSII^{-1}$·s^{-1} in the PSI deleted ΔAB cells, when the CO_2 assimilation rate in the darkness was surprisingly as high as 5±2 mol CO_2·mol $PSII^{-1}$·s^{-1}. The light-minus-dark CO_2 assimilation rate in the ΔAB cells was likely under-estimated because the dilution of $^{14}CO_2$ as a result of the release of non-labeled CO_2 by respiration was ignored in the analysis. This notion was supported by the increase of the measured light-minus-dark CO_2 assimilation rate of the WT cells from 16±7 mol CO_2·mol $PSII^{-1}$·s^{-1} to 34±6 mol CO_2·mol $PSII^{-1}$·s^{-1} when the reaction media were changed from those containing 5 mM glucose to those without glucose. Therefore, we conclude that the PSI deleted ΔAB cells assimilate CO_2 at a significant rate as compared to the O_2 evolution rates: The light-minus-dark CO_2 assimilation rate (2.2±0.9 mol CO_2·mol $PSII^{-1}$·s^{-1}) is at least 55% of the light-minus-dark O_2 evolution rate (4±1 mol O_2·mol $PSII^{-1}$·s^{-1}).

We tested the effects of the electron transport inhibitors and glucose deprivation on CO_2 assimilation of the ΔPSI cells. Our data show that the light-minus-dark CO_2 assimilation rate was inhibited by 10 μM DCMU (90% inhibition) or 1 mM KCN (100% inhibition). In addition, the light-minus-dark CO_2 assimilation rate dropped upon glucose deprivation and recovered upon adding back glucose (e.g., in one experiment, the light-minus-dark CO_2 assimilation rate dropped to 29% after 24 h glucose deprivation and recovered to 66% after adding back glucose for 3.5 h). The similarity between the light-minus-dark CO_2 assimilation and O_2 evolution in their responses to the electron transport inhibitors and glucose deprivation indicates that the observed light-minus-dark CO_2 assimilation of the

ΔPSI cells is a key PQH_2-oxidizing pathway enabling the net light-induced O_2 evolution in the ΔPSI cells.

4. Discussion

In this paper, we have demonstrated the following new observations: (1) a net light-induced O_2 evolution is present in the *Synechocystis* 6803 cells lacking PSI; (2) this net light-induced O_2 evolution of the ΔPSI cells requires glucose and can be sustained for over 30 min; (3) the rate of net light-induced O_2 evolution (P_{obs}) of the ΔPSI cells is ca. 13% of the WT rate on a PSII basis; (4) this net light-induced O_2 evolution of the ΔPSI cells is driven by PSII and the pathway of electrons includes the PQ pool but not the Q_o site of the Cyt bf complex; and (5) this net light-induced O_2 evolution of the ΔPSI cells is highly sensitive to KCN addition.

We also looked for the terminal electron acceptor pools of this PSI-independent, net light-induced O_2 evolution. As will be discussed below, we suggest that CO_2, but not the PQ pool or O_2, is a key terminal electron acceptor. A working model depicting O_2 evolving electron transport and CO_2 assimilation in the ΔPSI cells is proposed in Fig. 8B.

First, with the limited size of the PQ pool (ca. 10 molecules·$PSII^{-1}$)[34], all PQ molecules can be reduced within 2 s. Therefore, our observation that the ΔPSI cells could sustain the net light-induced O_2 evolution for 30 min at a rate as high as 4±1 O_2·$PSII^{-1}$·s^{-1} strongly argues against the hypothesis of Smart *et al.*[8] that the PQ pool serves as the main terminal electron acceptor for the net light-induced O_2 evolution in the ΔPSI cells.

Second, O_2 is a logical candidate to be an electron sink for the PQH_2-oxidizing pathway(s) in the PSI deletion mutants of *Synechocystis* 6803, as respiration and photosynthesis in cyanobacteria share common components such as the Cyt bf complex, the PQ pool and NADPH[48]. Vermaas et al.[20] and Vermaas[19] suggested that a respiratory terminal oxidase may direct the electrons generated by PSII to O_2 in the ΔPSI/WV cells. Notably different from our results, Vermaas[19] showed that the ΔPSI/WV cells did not display net O_2 evolution in the light. However, we observed net light-induced O_2 evolution in the ΔPSI (including ΔPSI/WV) cells; if all the PSII-generated electrons were directed to O_2, there would have been no net O_2 evolution[49–52]. Thus, to explain our data, other electron acceptors must also exist (see the Supplemental Material S2 for preliminary data and an elaborated discussion). We speculate that this discrepancy may be due to the differences in growth conditions, including light intensities and glucose concentrations**. Of note, in this work, we primarily use the net light-induced O_2 evolution rate P_{obs} as the readout. However, because the O_2 evolution rate is classically calculated with adjustment for dark respiration (i.e., P_{adj}), we also report in this work P_{adj}, assuming that respiration does not change in light. As respiration and photosynthesis are imbricated in cyanobacteria, O_2 uptake possibly varies during the light phase in the ΔPSI cells. For instance, as a result of enhanced oxidase activity, which is likely in the absence of PSI, O_2 uptake in the light could be stimulated.

**Light intensities: 5 μmol photons·m^{-2}·s^{-1} for ΔPSI/WV and 1.5 μmol photons·m^{-2}·s^{-1} in the present work. Glucose concentrations: 15 mM for ΔPSI/WV and 5 mM in the present work.

Further, mass spectroscopic data exist on another cyanobacterium *Synechococcus elongatus* (previously known as *Anacystis nidulans*) that at medium and high light intensities, O_2 uptake is enhanced in the light[30]. If O_2 uptake in the light is indeed enhanced in the ΔPSI cells, true O_2 evolution in these cells would be much higher than reported by P_{obs}.

Third, we have further demonstrated that CO_2 may serve as a key terminal electron acceptor of the PQH_2-oxidizing pathway(s) in the ΔPSI cells: Upon illumination, the ΔPSI cells can assimilate CO_2 at a rate that accounts for ca. 55% of the net light-induced O_2 evolution rate, and this light-minus-dark CO_2 assimilation is DCMU- and KCN-sensitive. These observations were made in the presence of 5 mM glucose and 10 mM $NaHCO_3$. We also found that the O_2 evolution rate in the ΔPSI cells decreased when CO_2 was depleted by bubbling $NaHCO_3$-less BG-11 medium with air filtered through Soda Lime (containing >75% $Ca(OH)_2$ and <3.5% NaOH). This finding is consistent with CO_2 being a key terminal electron acceptor in the ΔPSI O_2 evolution pathway. In *Synechocystis*, it is known that CO_2 assimilation is intertwined with a network of carbon metabolism. In this network, glycolysis and the tricarboxylic acid (TCA) cycle are connected not only to the Calvin-Benson cycle, but also to the oxidative pentose phosphate pathway, the glyoxylate pathway and nitrogen storage. It is also known that TCA cycle is incomplete in *Synechocystis*, lacking 2-ketoglutarate dehydrogenase or 2-ketoglutarate ferredoxin oxidoreductase[53]. Based on our pilot studies (see Supplemental Material S3) that attempted to address the mechanism responsible for the net light-induced O_2 evolution and the light-minus-dark CO_2 assimilation in the ΔPSI cells and the reported metabolic flux analysis showing the operation of a C_4-like pathway involving PEP carboxylase and malic enzyme in the mixotrophically-grown *Synechocystis* 6803 for the delivery of substantial carbon flow from the TCA cycle to the glycolysis pathway[54], we speculate that (1) the CO_2-assimilating PQH_2-oxidizing pathway in the ΔPSI cells may involve a glycolysis-dependent pathway with a glucose metabolite serving as the immediate electron acceptor after the PQ pool, but not the Calvin-Benson cycle or the cyanophycin synthesis pathway that assimilates both carbon and nitrogen at the same time; and (2) the alternative glycolysis-dependent CO_2-assimilating pathway in the ΔPSI cells may involve fumarate generation via PEP carboxylase/malic enzyme and subsequent fumarate reduction via succinate dehydrogenase working in reverse (Fig. 8B) (see Supplemental Material S3 for preliminary data and an elaborate discussion).

Finally, our efforts to identify additional terminal electron acceptor pools (e.g., H^+) (see Supplemental Material S4) were unsuccessful. Due to the complex nature of this newly discovered alternative PQH_2-oxidizing pathways in the ΔPSI cells, we suggest that techniques such as mass spectrometry-based metabolic flux analysis utilizing isotopically labeled O_2/CO_2 and GC/MS[54–55] as well as genomic and/or proteomic studies will be particularly valuable to dissect the intercalated network of the metabolite pools and enzymes for the final solution of the mechanism of the net light-induced O_2 evolution in PSI deletion mutants of the cyanobacterium *Synechocystis* sp. PCC 6803.

Highlights

- Synechocystis mutants lacking Photosystem I are able to produce oxygen in light

- This occurs in mixotrophically grown cells and in the presence of glucose
- This oxygen evolution requires Photosystem II and plastoquinone pool
- A KCN-sensitive pathway exists for this oxygen evolution to occur
- It is accompanied by low CO_2 assimilation; an alternate pathway must exist

Supplementary Material

Refer to Web version on PubMed Central for supplementary material.

Acknowledgement

We thank Himadri Pakrasi for providing us with the ΔVIII–XI and ΔAB mutant strains, and Wim F. J. Vermaas for the ΔPSIΔApcE, ΔPSIΔNdbABC, and ΔPSIΔCtaDIIEIIΔCydAB mutant strains. Q.J.W. thanks Elena Zak for her help. We thank Archie Portis, Donald Ort, David Krogmann, William Cramer, Aaaron Kaplan, Jean-David Rochaix and Kevin Redding for helpful discussions. We also thank Lawrence B. Smart for sharing his unpublished results. Finally, we give special thanks to Wim F. J. Vermaas for discussions that led to significant improvement of this paper.

Abbreviations

Chl	chlorophyll
PSII	photosystem II
Cyt bf	cytochrome b_6f
Cyt c_6	cytochrome c_6
PSI	photosystem I
Fd	ferredoxin
FNR	ferredoxin-$NADP^+$-oxidoreductase
Pheo	pheophytin
FQR	ferredoxin-plastoquinone-oxidoreductase
PQ	plastoquinone
PQH_2	plastoquinol
P680	special pair of Chl *a* molecules for primary photochemistry in PSII
P700	special pair of Chl *a* molecules for primary photochemistry in PSI
Q_A	first plastoquinone electron acceptor of PSII
Q_B	second plastoquinone electron acceptor of PSII
Q_o	the plastoquinol oxidase site of the Cyt bf complex
DCMU	3-(3,4-dichlorophenyl)-1,1-dimethylurea

KCN	potassium cyanide
FeCN	potassium ferricyanide
DCBQ	2,6-dichloro-*p*-benzoquinone
DBMIB	2,5-dibromo-3-methyl-6-isopropyl-*p*-benzoquinone
DCPIP	2,6-dichlorophenolindophenol
MV	methyl viologen
WT	wild type
ΔPSI	PSI deletion
PEP	phosphoenol pyruvate
Rubisco	ribulose-1,5-bisphosphate carboxylase/oxygenase

References

1. Duysens LN, Amesz J, Kamp BM. Two photochemical systems in photosynthesis. Nature. 1961; 190: 510–511. [PubMed: 13725322]
2. Hill R, Bendall F. Function of the two cytochrome components in chloroplasts - a working hypothesis. Nature. 1960; 186: 136–137.
3. Blankenship, R. Molecular Mechanisms of Photosynthesis. Oxford: Blackwell Science; 2002.
4. Wydrzynski, TJ, Satoh, K. Advances in photosynthesis and respiration series. The Netherland: Springer, Dordrecht; 2006. Photosystem II: The light-driven waterplastoquinone oxidoreductase.
5. Golbeck, JH. Advances in photosynthesis and respiration series. The Netherlands: Springer, Dordrecht; 2006. Photosystem I: The light-driven plastocyanin:ferredoxin oxidoreductase.
6. Cramer WA, Zhang H. Consequences of the structure of the cytochrome b6f complex for its charge transfer pathways. Biochim Biophys Acta. 2006; 1757: 339–345. [PubMed: 16787635]
7. Govindjee, Munday JC Jr, Papageorgiou G. Fluorescence studies with algae: changes with time and preillumination. Brookhaven Symp Biol. 1966; 19: 434–445. [PubMed: 5969947]
8. Smart LB, Anderson SL, McIntosh L. Targeted genetic inactivation of the photosystem I reaction center in the cyanobacterium *Synechocystis* sp. PCC 6803. EMBO J. 1991; 10: 3289–3296. [PubMed: 1717264]
9. Arnon DI. Divergent pathways of photosynthetic electron transfer: The autonomous oxygenic and anoxygenic photosystems. Photosynth Res. 1995; 46: 47–71. [PubMed: 24301568]
10. Peltier G, Cournac L. Chlororespiration. Annu Rev Plant Biol. 2002; 53: 523–550. [PubMed: 12227339]
11. Cournac L, Redding K, Bennoun P, Peltier G. Limited photosynthetic electron flow but no CO_2 fixation in *Chlamydomonas* mutants lacking photosystem I. FEBS Lett. 1997; 416: 65–68. [PubMed: 9369234]
12. Cournac L, Redding K, Ravenel J, Rumeau D, Josse EM, Kuntz M, Peltier G. Electron flow between photosystem II and oxygen in chloroplasts of photosystem I-deficient algae is mediated by a quinol oxidase involved in chlororespiration. J Biol Chem. 2000; 275: 17256–17262. [PubMed: 10748104]
13. Redding K, Cournac L, Vassiliev IR, Golbeck JH, Peltier G, Rochaix J-D. Photosystem I is indispensable for photoautotrophic growth CO_2 fixationand H_2 photoproduction in *Chlamydomonas reinhardtii*. J Biol Chem. 1999; 274: 10466–10473. [PubMed: 10187837]

14. Boussiba, S, Vermaas, WFJ. Creation of a mutant with an enriched photosystem II/pigment ratio in the cyanobacterium *Synechocystis* sp. PCC 6803. In: Murata, N, editor. Research in Photosynthesis. 1992. 429–432.
15. Shen G, Boussiba S, Vermaas WFJ. *Synechocystis* sp PCC 6803 strains lacking photosystem I and phycobilisome function. Plant Cell. 1993; 5: 1853–1863. [PubMed: 8305875]
16. Howitt CA, Udall PK, Vermaas WFJ. Type 2 NADH dehydrogenases in the cyanobacterium *Synechocystis* sp. strain PCC 6803 are involved in regulation rather than respiration. J Bacteriol. 1999; 181: 3994–4003. [PubMed: 10383967]
17. Howitt CA, Vermaas WFJ. Quinol and cytochrome oxidases in the cyanobacterium *Synechocystis* sp. PCC 6803. Biochemistry. 1998; 37: 17944–17951. [PubMed: 9922162]
18. Berry S, Schneider D, Vermaas WFJ, Rogner M. Electron transport routes in whole cells of *Synechocystis* sp. strain PCC 6803: the role of the cytochrome *bd*-type oxidase. Biochemistry. 2002; 41: 3422–3429. [PubMed: 11876651]
19. Vermaas WFJ. Molecular-genetic approaches to study photosynthetic and respiratory electron transport in thylakoids from cyanobacteria. Biochim. Biophys. Acta. 1994; 1187: 181–186.
20. Vermaas WFJ, Shen G, Styring S. Electrons generated by photosystem II are utilized by an oxidase in the absence of photosystem I in the cyanobacterium *Synechocystis* sp. PCC 6803. FEBS Lett. 1994; 337: 103–108. [PubMed: 8276100]
21. Zhang L, McSpadden B, Pakrasi HB, Whitmarsh J. Copper-mediated regulation of cytochrome c_{553} and plastocyanin in the cyanobacterium *Synechocystis* 6803. J Biol Chem. 1992; 267: 19054–19059. [PubMed: 1326543]
22. Williams JGK. Construction of specific mutations in photosystem II photosynthetic reaction center by genetic engineering methods in *Synechocystis* 6803. Methods Enzymol. 1988; 167: 766–778.
23. Nedbal L, Gibas C, Whitmarsh J. Light saturation curves show competence of the water splitting complex in inactive photosystem II reaction centers. Photosynth Res. 1991; 30: 85–94. [PubMed: 24415257]
24. Mannan RM, Whitmarsh J, Nyman P, Pakrasi HB. Directed mutagenesis of an iron-sulfur protein of the photosystem I complex in the filamentous cyanobacterium *Anabaena variabilis* ATCC 29413. Proc Natl Acad Sci U S A. 1991; 88: 10168–10172. [PubMed: 1658798]
25. Nyhus KJ, Ikeuchi M, Inoue Y, Whitmarsh J, Pakrasi HB. Purification and characterization of the photosystem I complex from the filamentous cyanobacterium *Anabaena variabilis* ATCC 29413. J Biol Chem. 1992; 267: 12489–12495. [PubMed: 1618755]
26. Porra RJ, Thompson WA, Kriedemann PE. Determination of accurate extinction coefficients and simultaneous equations for assaying chlorophylls a and b extracted with four different solvents: Verification of the concentration of chlorophyll standards by atomic absorption spectroscopy. Biochim. Biophys. Acta. 1989; 975: 384–394.
27. Mannan RM, He WZ, Metzger SU, Whitmarsh J, Malkin R, Pakrasi HB. Active photosynthesis in cyanobacterial mutants with directed modifications in the ligands for two iron-sulfur clusters on the PsaC protein of photosystem I. EMBO J. 1996; 15: 1826–1833. [PubMed: 8617228]
28. Trtílek M, Kramer DM, Koblížek M, Nedbal L. Dual-modulation LED kinetic fluorometer. J Luminescence. 1997; 72–74: 597–599.
29. Eckardt NA, Snyder GW, Portis AR Jr, Orgen WL. Growth and photosynthesis under high and low irradiance of *Arabidopsis thaliana* antisense mutants with reduced ribulose-1,5-bisphosphate carboxylase/oxygenase activase content. Plant Physiol. 1997; 113: 575–586. [PubMed: 9046598]
30. Hoch G, Owens OV, Kok B. Photosynthesis and respiration. Arch Biochem Biophys. 1963; 101: 171–180. [PubMed: 13954893]
31. Rippka R, Deruelles J, Waterbury JB, Herdman M, Stanier RY. Generic assignments, strain histories and properties of pure cultures of cyanobacteria. J Gen Microbiol. 1979; 111: 1–61.
32. Kahlon S, Beeri K, Ohkawa H, Hihara Y, Murik O, Suzuki I, Ogawa T, Kaplan A. A putative sensor kinase, Hik31, is involved in the response of *Synechocystis* sp. strain PCC 6803 to the presence of glucose. Microbiology. 2006; 152: 647–655. [PubMed: 16514145]
33. Govinjee. Sixty-three years since Kautsky. Aust J Plant Biol (now Funct Plant Biol). 1995; 22: 131–160.

34. Papageorgiou, GC, Govindjee. Advances in photosynthesis and respiration series. The Netherlands: Springer, Dordrecht; 2005. Chlorophyll *a* fluorescence: A signature of photosynthesis.
35. Duysens, LNM, Sweers, HE. Studies on Microalgae and Photosynthetic Bacteria., Japanese Soc Plant Physiol. Tokyo: University of Tokyo Press; 1963. Mechanism of the two photochemical reactions in algae as studied by means of fluorescence; 353–372.
36. Koblížek M, Kaftan D, Nedbal L. On the relationship between the non-photochemical quenching of the chlorophyll fluorescence and the photosystem II light harvesting efficiency. A repetitive flash fluorescence induction study. Photosynth Res. 2001; 68: 141–152. [PubMed: 16228337]
37. Mi H, Endo T, Ogawa T, Asada K. Thylakoid membrane-bound, NADPH-specific pyridine nucleotide dehydrogenase complex mediates cyclic electron transport in the cyanobacterium *Synechocystis* sp. PCC 6803. Plant Cell Physiology. 1995; 36: 661–668.
38. Mi H, Endo T, Schreiber U, Ogawa T, Asada K. NAD(P)H dehydrogenase-dependent cyclic electron flow around photosystem I in the cyanobacterium *Synechocystis* PCC 6803: a study of dark-starved cells and spheroplasts. Plant Cell Physiology. 1994; 35: 163–173.
39. Jones RW, Whitmarsh J. Inhibition of electron transfer and the electrogenic reaction in the cytochrome b/f complex by 2-n-nonyl-4-hydroxyquinoline N-oxide (NQNO) and 2,5-dibromo-3-methyl-6-isopropyl-p-benzoquinone (DBMIB). Biochim. Biophys. Acta. 1988; 933: 258–268.
40. Trebst A. Inhibitors in electron flow: tools for the functional and structural localization of carriers and energy conservation sites. Methods Enzymol. 1980; 69: 675–715.
41. Ouitrakul R, Izawa S. Electron transport and photophosphorylation in chloroplasts as a function of the electron acceptor. II. Acceptor-specific inhibition by KCN. Biochim Biophys Acta. 1973; 305: 105–118. [PubMed: 4719594]
42. Wishnick M, Lane MD. Inhibition of ribulose diphosphate carboxylase by cyanide. Inactive ternary complex of enzyme, ribulose diphosphate, and cyanide. J Biol Chem. 1969; 244: 55–59. [PubMed: 5773288]
43. Charles AM, White B. Ribulose biophosphate carboxylase from *Thiobacillus A2*. Its purification and properties. Arch Microbiol. 1976; 108: 195–202. [PubMed: 5983]
44. Badger MR, Price GD. CO_2 concentrating mechanisms in cyanobacteria: molecular components, their diversity and evolution. J Exp Bot. 2003; 54: 609–622. [PubMed: 12554704]
45. Kaplan A, Reinhold L. CO_2 concentrating mechanisms in photosynthetic microorganisms. Annu Rev Plant Physiol Plant Mol Biol. 1999; 50: 539–570. [PubMed: 15012219]
46. Moroney JV, Somanchi A. How do algae concentrate CO_2 to increase the efficiency of photosynthetic carbon fixation? Plant Physiol. 1999; 119: 9–16. [PubMed: 9880340]
47. Price GD, Maeda SI, Omata T, Badger MR. Modes of active inorganic carbon uptake in the cyanobacterium, *Synechocystis* sp. PCC7942. Funct Plant Biol. 2002; 29: 131–149. [PubMed: 32689461]
48. Schmetterer, G. Cyanobacterial respiration. In: Bryant, DA, editor. The Molecular Biology of Cyanobacteria. The Netherlands: Kluwer Academic Publishers; 1994. 409–435.
49. Yamamoto H, Miyake C, Dietz K, Tomizawa K, Murata N, Yokota A. Thioredoxin peroxidase in the cyanobacterium *Synechocystis* sp. PCC 6803. FEBS Lett. 1999; 447: 269–273. [PubMed: 10214959]
50. Asada K. The water-water cycle in chloroplasts: scavenging of active oxygens and dissipation of excess photons. Annu Rev Plant Physiol Plant Mol Biol. 1999; 50: 601–639. [PubMed: 15012221]
51. Miyake C, Michihata F, Asada K. Scavenging of hydrogen peroxide in prokaryotic and eukaryotic algae: Acquisition of ascorbate peroxidase during the evolution of cyanobacteria. Plant Cell Physiol. 1991; 52: 33–43.
52. Asada K. Production and scavenging of reactive oxygen species in chloroplasts and their functions. Plant Physiol. 2006; 141: 391–396. [PubMed: 16760493]
53. Huynen MA, Dandekar T, Bork P. Variation and evolution of the citric-acid cycle: a genomic perspective. Trends Microbiol. 1999; 7: 281–291. [PubMed: 10390638]
54. Yang C, Hua Q, Shimizu K. Metabolic flux analysis in *Synechocystis* using isotope distribution from ^{13}C-labeled glucose. Metab Eng. 2002; 4: 202–216. [PubMed: 12616690]

55. Helman Y, Barkan E, Eisenstadt D, Luz B, Kaplan A. Fractionation of the three stable oxygen isotopes by oxygen-producing and oxygen-consuming reactions in photosynthetic organisms. Plant Physiol. 2005; 138: 2292–2298. [PubMed: 16040650]

56. Munday JC Jr, Govindjee. Light-induced changes in the fluorescence yield of chlorophyll A *in vivo*. III. The dip and the peak in the fluorescence transient of *Chlorella pyrenoidosa*. Biophys J. 1969; 9: 1–21. [PubMed: 5782892]

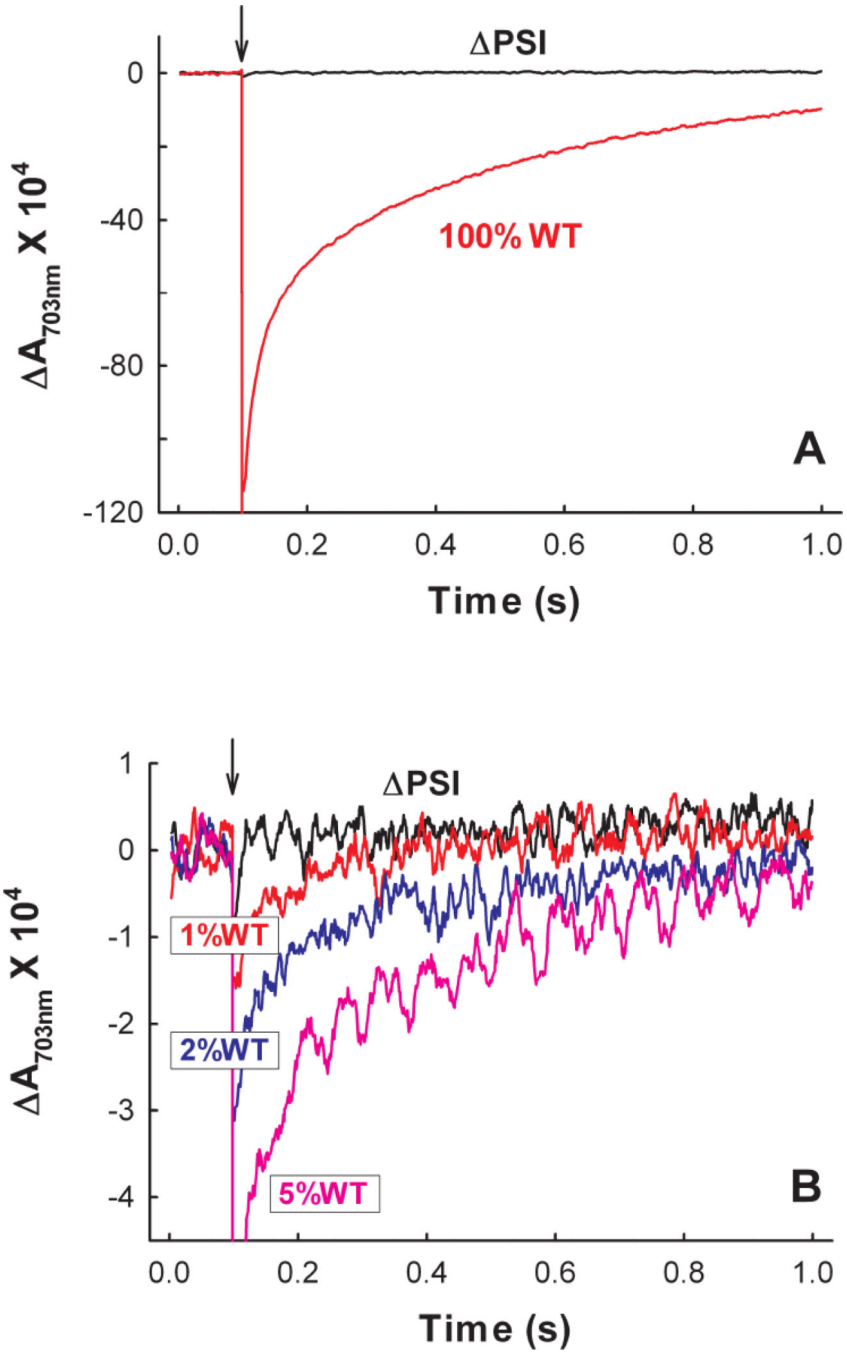

Figure 1. The absence of PSI in the PSI deleted ΔAB mutant strain of *Synechocystis* 6803 is confirmed by the lack of P700 oxidation-induced absorbance change at 703 nm in the ΔAB membrane preparation

(A) Absorption transient at 703 nm reflecting the P700 oxidation and re-reduction kinetics of the WT *Synechocystis* 6803 membranes and lack of it in the ΔAB membranes. **(B)** Absorption transient at 703 nm (on an expanded scale) demonstrating the lack of the P700 response in the ΔAB membranes as compared to that of the ΔAB membranes with 1%, 2% and 5% WT admixtures. In both (**A**) and (**B**), the arrows indicate the times when the actinic

flashes were fired. The reaction buffer contained 50 mM Tris-HCl (pH 8.3), 33 μM DCPIP, 1.7 mM sodium ascorbate and 50 nM PSII. The experiments were carried out at 24±1°C.

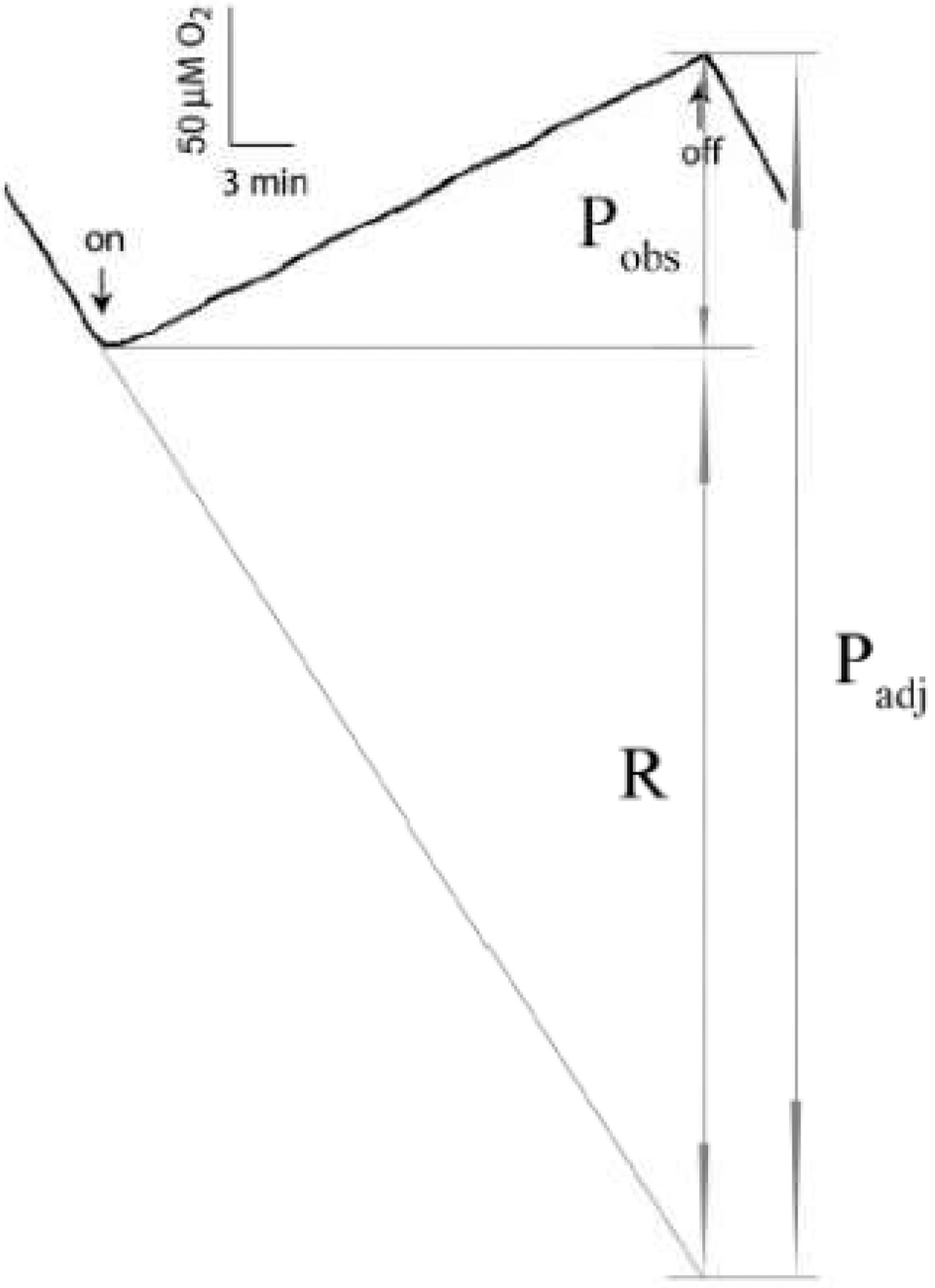

Figure 2. A typical chart recorder trace of the light-induced O_2 evolution of the ΔPSI (ΔAB) cells in the presence of 5 mM glucose and 10 mM $NaHCO_3$

The rates of the dark respiration (R) and of the light-induced O_2 evolution either with (P_{adj}) or without (P_{obs}) adjustment for dark respiration are labeled. The down- and up-arrows indicate the times when the actinic light was turned on and off, respectively. This figure shows that the ΔAB cells were able to maintain substantial and constant rates of net light-induced O_2 evolution P_{obs} for 30 min. The Chl concentration of this sample was 1.3 μM. The experiment was carried out at 30°C.

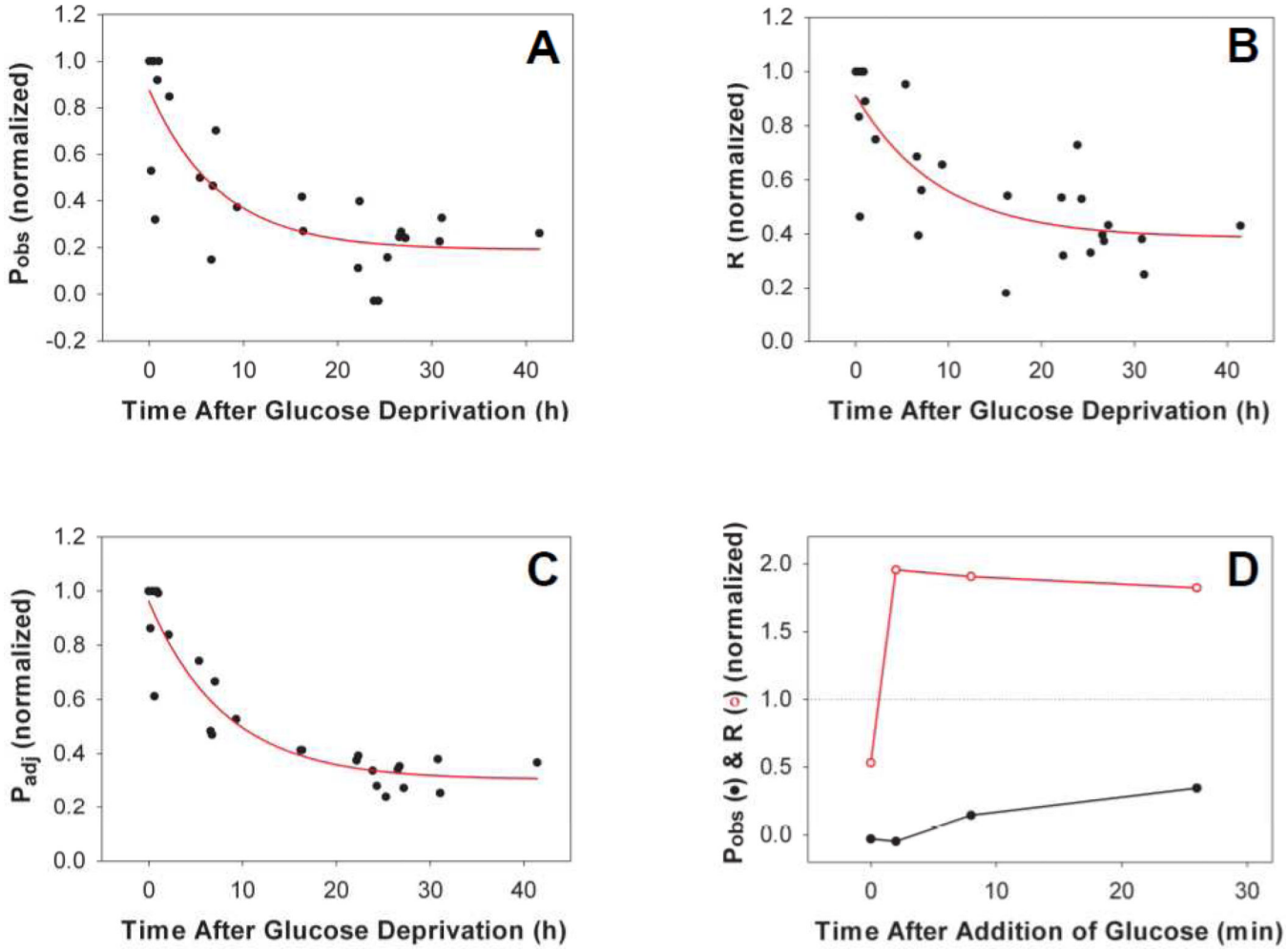

Figure 3. Requirement of glucose for both O_2 evolution and dark respiration in the ΔPSI (ΔAB) mutant

The net light-induced O_2 evolution rate P_{obs} **(A)**, dark respiration rate R **(B)** and the adjusted O_2 evolution rate P_{adj} **(C)** of the ΔAB cells dropped gradually after glucose deprivation (time constant ca. 8 h). The exponentially grown cells were harvested, washed and re-suspended in fresh BG-11 medium without glucose and kept at 30°C and under 1 μmol photons·$m^{-2}s^{-1}$ light prior to experiments. A final concentration of 10 mM $NaHCO_3$ was added before each measurement. For each panel, data from 3 independent experiments were normalized to the maximal rate (right before glucose deprivation) and combined. For each rate, 100% activity is the activity before the sample was deprived of glucose. **(D)** Recovery of the net light-induced O_2 evolution rate (P_{obs}) (closed circles) and the dark respiration rate (R) (open circles) after glucose (5 mM) was supplied to the 42 h glucose-depleted ΔAB cells. Since 5 mM glucose was enough to maintain cell growth until stationary phase, the remaining glucose concentration during/after the measurements was assumed to be sufficient.

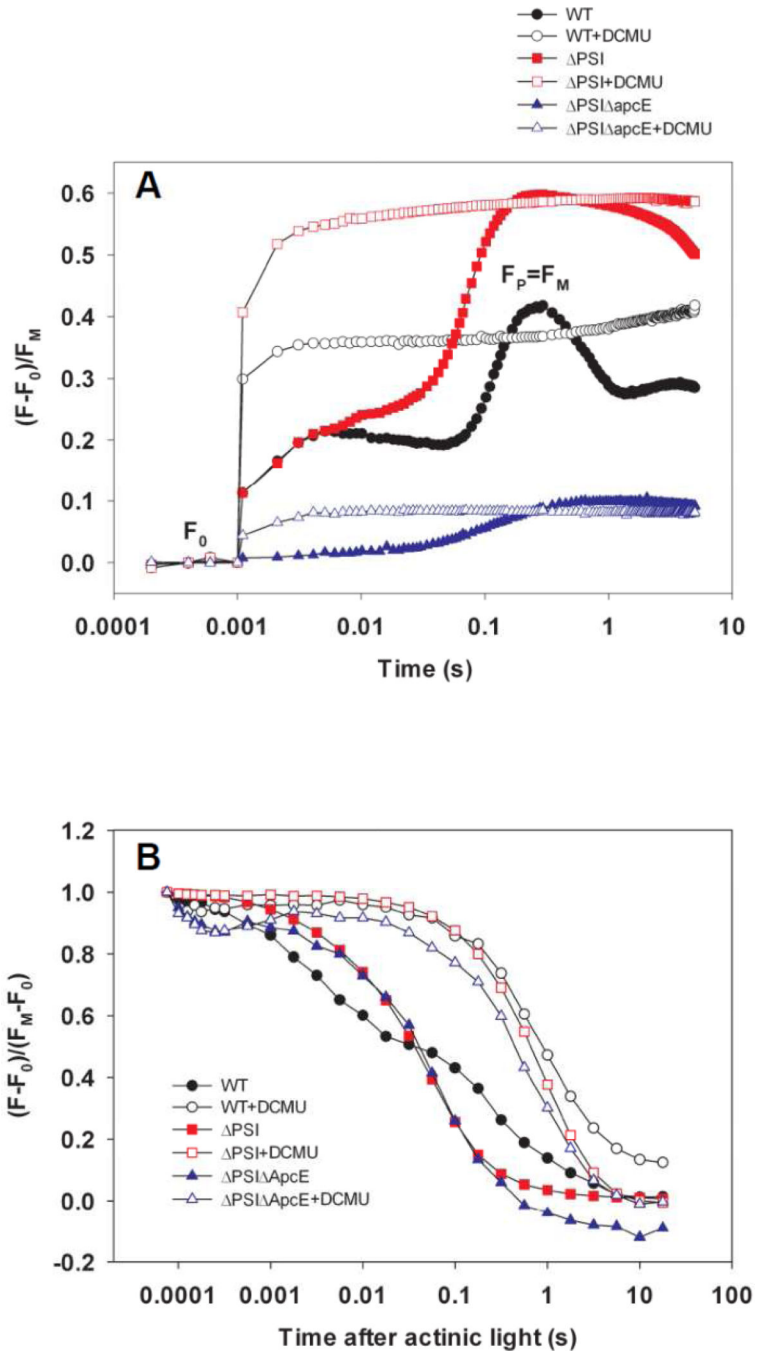

Figure 4. DCMU effects on Chl *a* fluorescence kinetics of the WT and the ΔPSI cells

(**A**) Chl *a* fluorescence induction curves of the WT (circles), ΔAB (squares, labeled as ΔPSI) and ΔPSIΔApcE (triangles) cells show the same effect of DCMU on the WT and ΔPSI cells: The illumination time needed to fully reduce Q_A decreased from hundreds of milliseconds (WT: 170 ms; ΔAB: 320 ms; ΔPSIΔApcE: 560 ms) in the absence of DCMU to 2 milliseconds or less when DCMU is present. (**B**) Chl *a* fluorescence dark relaxation curves of the WT (circles), ΔAB (squares, labeled as ΔPSI) and ΔPSIΔApcE (triangles) cells show the same slow kinetics in both the WT and ΔPSI cells in the presence of DCMU (open

symbols, $T^{DCMU} \approx 1$ s) and yet there is drastically different kinetics between the WT (black closed circles, bi-phasic, $T_{slow}{}^{WT} = 0.1–1$ s and $T_{fast}{}^{WT} \approx 1–10$ ms) and ΔPSI (red closed squares for ΔAB and blue closed triangles for ΔPSIΔApcE, monophasic, $T^{\Delta PSI} \approx 10–100$ ms) cells in the absence of DCMU. In both (**A**) and (**B**), a total of 370 saturating actinic flashes were given at the frequency of 1 kHz to maximally reduce Q_A and the PQ pool prior to recording the dark relaxation kinetics. The time when the actinic flashes were turned off was set as zero. DCMU was applied at a final concentration of 10 μM.

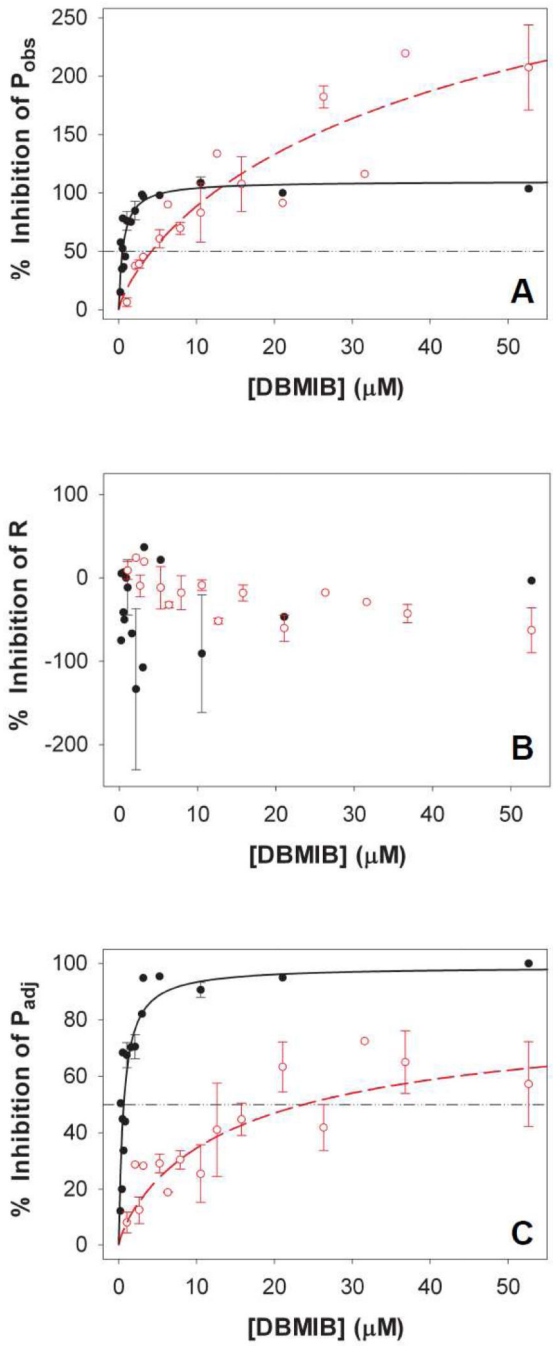

Figure 5. DBMIB titration of (A) P_{obs}, (B) R and (C) P_{adj} of the WT and the ΔPSI cells

P_{obs} and P_{adj} of the ΔPSI cells were significantly less sensitive to DBMIB than those of the WT cells, whereas the rates of R in both the WT and the ΔPSI cells were not sensitive to DBMIB. The I_{50} values for DBMIB inhibition were 0.5 μM for P_{obs} of the WT cells (Panel A, black closed circles), 4.2 μM for P_{obs} of the ΔPSI cells (Panel A, red open circles), 0.6 μM for P_{adj} of the WT cells (Panel C, black closed circles), and 23.7 μM for P_{adj} of the ΔPSI cells (Panel C, red open circles). P_{obs}, R and P_{adj} of both the WT and ΔPSI cells were measured in BG-11 medium in the presence of 5 mM glucose and 10 mM

$NaHCO_3$. The titration curves of the WT cells (black closed circles) are plotted from 3 data sets. The titration curves of the ΔPSI cells (red open circles, for ΔAB, ΔVIII–XI, and ΔPSI/WV strains) are plotted from 4 data sets. Standard errors are indicated. In addition, we grew the ΔPSI cells either in the presence or in the absence of 1 μM Cu^{2+} supplement so that they expressed either plastocyanin or Cyt c_6, respectively [21]. Both plastocyanin- and Cyt c_6-expressing ΔPSI cells exhibited indistinguishable DBMIB titration curves: The data shown include those from cells grown both with and without Cu^{2+} supplement. For each rate, 100% inhibition by DBMIB means the rate is reduced from the control value (with no DBMIB) to zero. An inhibition that is greater than 100% in the case of P_{obs} means that in the presence of DBMIB, the cells show net O_2 consumption instead of displaying net O_2 evolution.

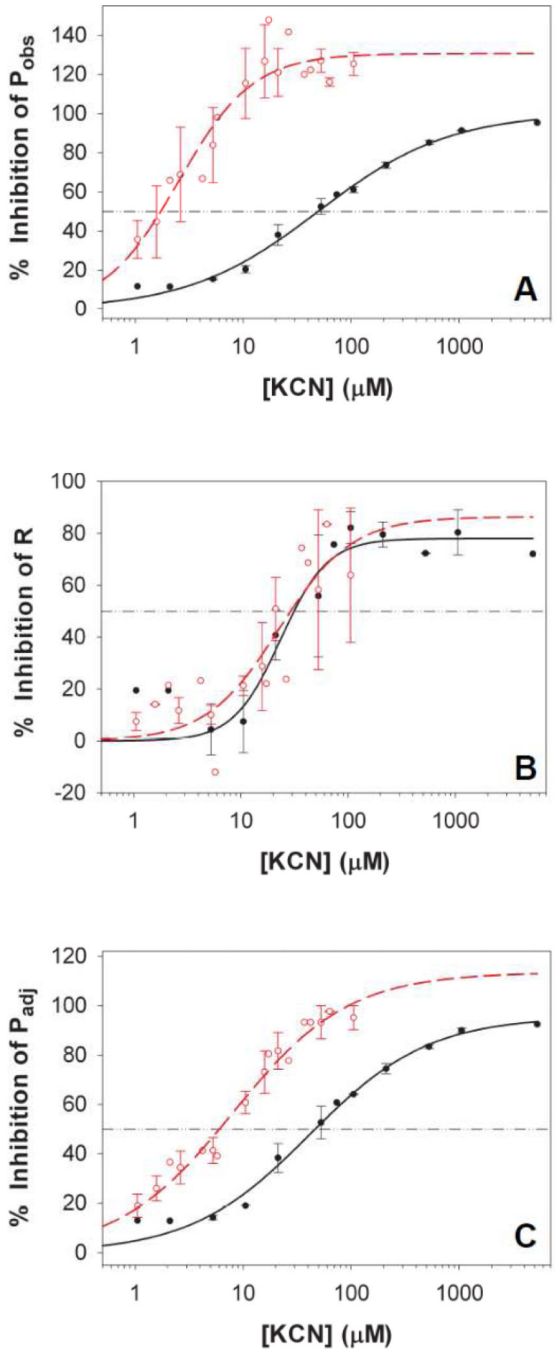

Figure 6. KCN titration of (A) P_{obs}, (B) R and (C) P_{adj} of the WT and the ΔPSI cells

P_{obs} and P_{adj} of the ΔPSI cells were much more sensitive to KCN than those of the WT cells, whereas R of the ΔPSI cells had the same sensitivity to KCN as that of the WT cells. The I_{50} values for KCN inhibition were 49 μM for P_{obs} of the WT cells (Panel A, black closed circles), 1.7 μM for P_{obs} of the ΔPSI cells (Panel A, red open circles), 46 μM for P_{adj} of the WT cells (Panel C, black closed circles), 6 μM for P_{adj} of the ΔPSI cells (Panel C, red open circles) and 30 μM for R of both the WT (Panel B, black closed circles) and ΔPSI (Panel B, red open circles) cells. P_{obs}, R and P_{adj} of both the WT and the ΔPSI cells were measured in

BG-11 medium in the presence of 5 mM glucose and 10 mM $NaHCO_3$. The titration curves of the WT cells (black closed circles) are plotted from 2 data sets. The titration curves of the ΔPSI cells (red open circles, for ΔAB, ΔVIII–XI, and ΔPSI/WV strains) are plotted from 5 data sets. Standard errors are indicated. In addition, the KCN sensitivities of both the WT and ΔPSI cells were not affected by the supplemental Cu^{2+} in the growth medium, as the data shown are for cells grown both with and without Cu^{2+} supplement. For each rate, 100% inhibition by KCN means the rate is reduced from the control value (with no KCN) to zero. An inhibition that is greater than 100% in the case of P_{obs} means that in the presence of KCN, the cells showed net O_2 consumption instead of displaying net O_2 evolution.

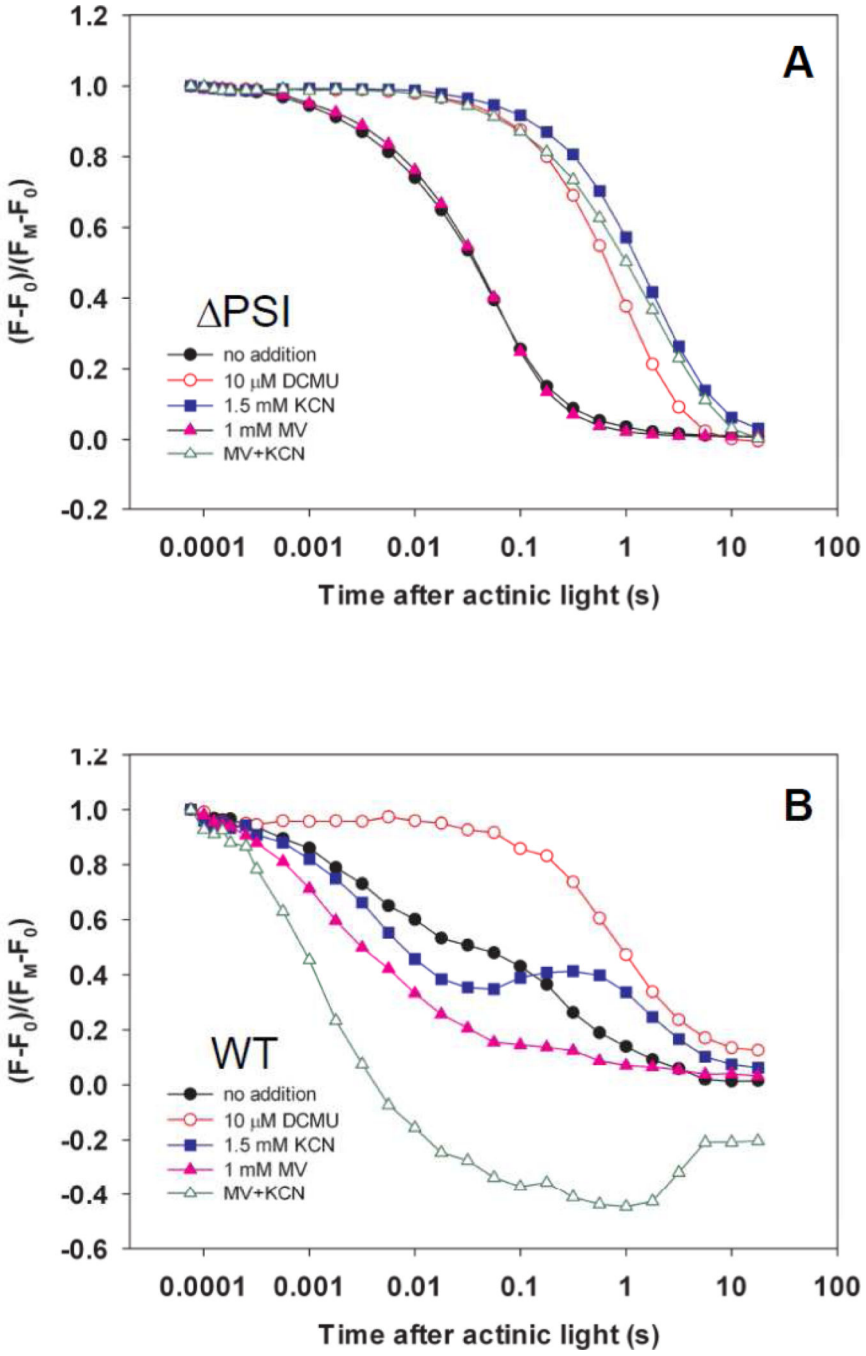

Figure 7. KCN effects on Chl *a* fluorescence dark relaxation kinetics of the (A) ΔPSI (ΔAB) and (B) WT cells

Like DCMU (Panel A, red open circles), KCN severely inhibited Chl *a* fluorescence dark relaxation in the ΔPSI cells (Panel A, blue closed squares), as compared to without KCN (Panel A, black closed circles), suggesting that KCN may effectively slow down the oxidation of Q_A^- and the PQH_2 pool in the ΔPSI cells. In contrast, in the WT cells, KCN did not cause inhibition of the PQH_2 pool oxidation; rather, it induced a small light-to-dark transient increase of the Chl *a* fluorescence yield (Panel B, blue closed squares) which was absent in the ΔPSI cells. This result is consistent with the lack of PSI and the cyclic electron

transport around PSI in the ΔPSI cells. This result was further supported by the capability of methylviologen (MV), an electron acceptor for PSI [56], to reverse the KCN inhibition of the PQH_2 pool oxidation in the WT cells (Panel B, green open triangles), but not in the ΔPSI cells (Panel A, green open triangles). In both (**A**) and (**B**), a total of 370 saturating actinic flashes were given at the frequency of 1 kHz to maximally reduce Q_A and the PQ pool prior to recording the dark relaxation kinetics. The time when the actinic flashes were turned off was set as zero. The concentrations of the inhibitors and electron acceptor used were as follows: 10 μM DCMU, 1.5 mM KCN, and 1 mM MV.

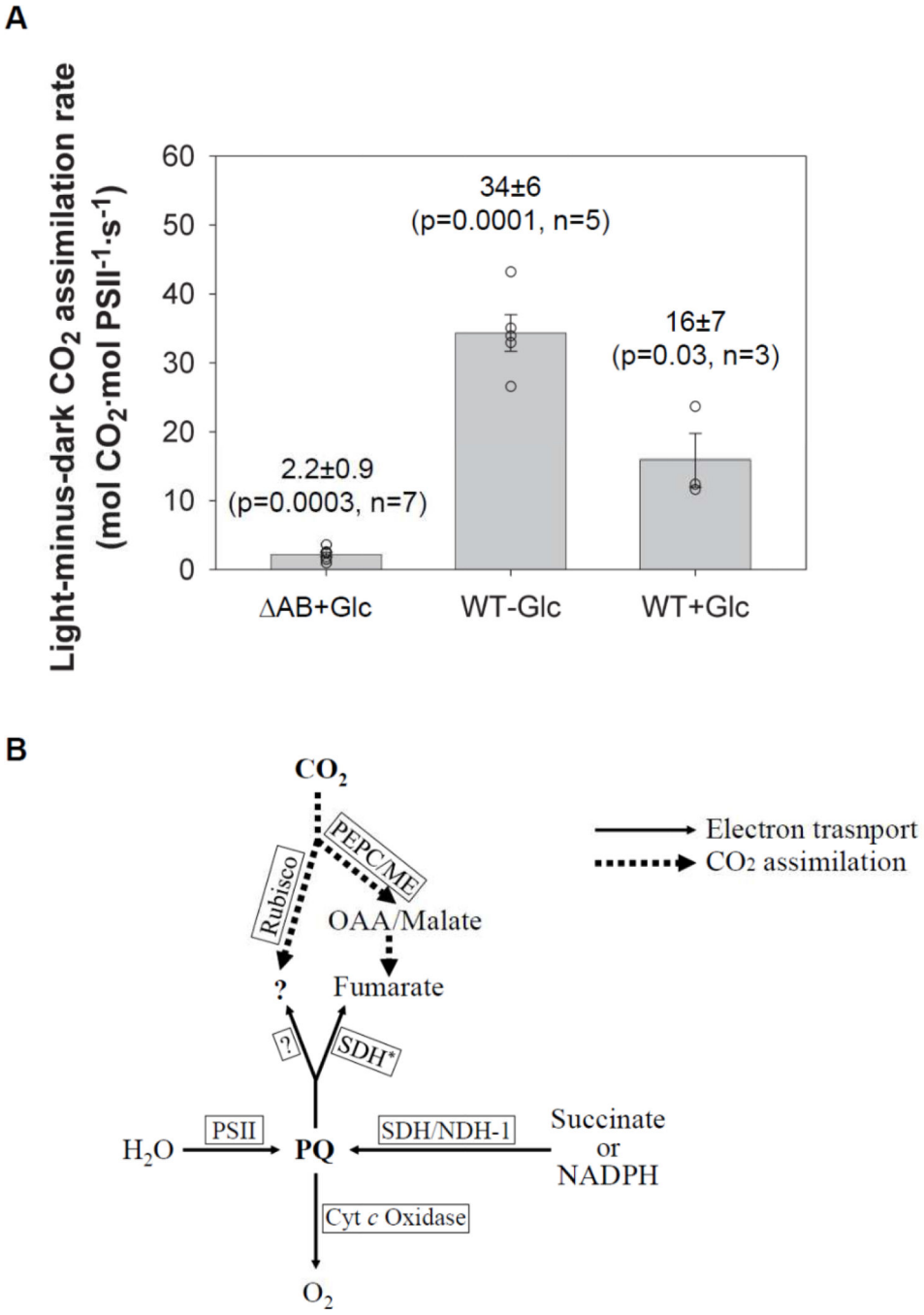

Figure 8. (A) The light-minus-dark CO_2 assimilation rates in the PSI deleted ΔAB and the WT cells in the presence of glucose and in the WT cells in the absence of glucose

Each experiment is represented by one open circle. The mean, the standard error, the p-value, and the number of independent experiments are indicated. The light-minus-dark CO_2 assimilation rates were calculated as the difference between the light and the dark CO_2 assimilation rates. Despite the high variation in the dark CO_2 assimilation rates, the light-minus-dark CO_2 assimilation rates are statistically highly significant, as evaluated by the paired t-test. **(B) The working model for the O_2 evolving electron transport (thin**

solid-line arrows) and light-minus-dark CO_2 assimilation (thick dotted-line arrows) in the ΔPSI cells. The PQ pool serves as the "hub" of the electron flows, with the incoming electrons from H_2O (via PSII) as well as succinate (via succinate dehydrogenase) and/or NADPH (via type 1 NAD(P)H dehydrogenase) and with the outgoing electrons to O_2 (via cytochrome *c* oxidases) and CO_2 (via Rubisco-dependent mechanisms and/or a glycolysis-dependent mechanism). The glycolysis-dependent CO_2 assimilation may involve PEP carboxylase and/or malic enzyme, which generate malate and/or oxaloacetate via carboxylation reactions, followed by a succinate dehydrogenase working in reverse as a fumarate reductase to reduce fumarate to succinate. All abbreviations used in this model are defined as follows: PSII – photosystem II, PQ – the plastoquinol pool, SDH – succinate dehydrogenase, SDH* – succinate dehydrogenase working in reverse as fumerate reductase, NDH-1 – type 1 NAD(P)H dehydrogenase, Cyt c oxidase – cytochrome c oxidase, OAA – oxaloacetate, PEPC – PEP carboxylase, ME – malic enzyme.

Table 1

The ΔPSI mutants used in this study.

Name	Mutation	Reference
ΔAB	A significant portion of the *psaAB* operon was deleted	E. Zak and H. Pakrasi, personal communication
ΔVIII–XI	A part of the *psaB* gene that encoded the VIIIth to XIth helices of the PsaB protein was deleted	E. Zak and H. Pakrasi, personal communication
ΔPSI/WV	PSI was deleted	[14]
ΔPSIΔApcE	Both PSI and the phycobilisome linker protein ApcE were deleted	[15]
ΔPSIΔNdbABC	Both PSI and the type 2 NADH dehydrogenase Ndb were deleted	[16]
ΔPSIΔCtaDIIEII ΔCydAB	Both PSI and the alternative terminal oxidases CtaII and Cyd were deleted	[17]

Table 2

Comparison of the O_2 evolution and CO_2 assimilation rates of *Synechocystis* 6803 WT (grown either in the absence or in the presence of 5 mM glucose, Glc) and the PSI deleted ΔAB (grown in the presence of 5 mM glucose) cells. Both the O_2 evolution and the CO_2 assimilation rates were measured in fresh BG-11 growth medium supplemented with 10 mM $NaHCO_3$ and the corresponding glucose content. As shown in Figure 2, P_{obs} is the net light-induced O_2 evolution rate obtained from the above-zero portion of the O_2 evolution traces and P_{adj} is the O_2 evolution rate adjusted for respiratory O_2 consumption, assuming that the respiration rate in the light is the same as in the dark (positive values for O_2 consumption). Since the ΔAB cells differed vastly from the WT cells in their Chl-to-PSII ratios, both the O_2 evolution and the CO_2 assimilation rates are normalized to the PSII content, utilizing the measured Chl-to-PSII ratios. The rates of corresponding electron fluxes can be obtained by multiplying the O_2 evolution rates by 4. The numbers of independent experiments preformed are indicated in parentheses. Detailed experimental conditions are described in **Materials and Methods**. Despite the high variation in the dark CO_2 assimilation rates, the light-minus-dark CO_2 assimilation rate is highly statistically significant, as examined by the paired t-test test (one-tailed, $p = 0.0003$) for 7 independent measurements.

Parameters measured	WT+Glc	WT-Glc	ΔPSI+Glc
Net O_2 evolution rate P_{obj} (mmol O_2·mol Chl^{-1}·s^{-1})	68 ± 10 (6)	82 ± 15 (7)	56 ± 14 (7)
Chl-to-PSII ratio	490 ± 25 (2)	518 (1)	78 ± 4 (2)
Net O_2 evolution rate P_{obj} (mol O_2·mol $PSII^{-1}$·s^{-1})	34 ± 5 (6)	42 ± 8 (7)	4 ± 1 (7)
Dark respiration rate R (mol O_2·mol $PSII^{-1}$·s^{-1})	5 ± 1 (6)	4 ± 2 (7)	6 ± 2 (7)
Adjusted O_2 evolution rate P_{adj} (mol O_2·mol $PSII^{-1}$·s^{-1})	39 ± 5 (6)	46 ± 8 (7)	10 ± 3 (7)
PSII activity (mol O_2·mol $PSII^{-1}$·s^{-1})	66 (1)	—	110 (1)
Dark CO_2 assimilation rate (mol CO_2·mol $PSII^{-1}$·s^{-1})	1.4 ± 0.7 (3)	1.4 ± 0.8 (5)	5 ± 2 (7)
Light-minus-dark CO_2 assimilation rate (mol CO_2·mol $PSII^{-1}$·s^{-1})	16 ± 7 (3)	34 ± 6 (5)	2.2 ± 0.9 (7)